Polarizations of J/ψ and $\psi(2S)$ Mesons Produced in $p\overline{p}$ Collisions at $\sqrt{s} = 1.96$ TeV

A. Abulencia,[24] J. Adelman,[13] T. Affolder,[10] T. Akimoto,[55] M.G. Albrow,[17] S. Amerio,[43] D. Amidei,[35] A. Anastassov,[52] K. Anikeev,[17] A. Annovi,[19] J. Antos,[14] M. Aoki,[55] G. Apollinari,[17] T. Arisawa,[57] A. Artikov,[15] W. Ashmanskas,[17] A. Attal,[3] A. Aurisano,[42] F. Azfar,[42] P. Azzi-Bacchetta,[43] P. Azzurri,[46] N. Bacchetta,[43] W. Badgett,[17] A. Barbaro-Galtieri,[29] V.E. Barnes,[48] B.A. Barnett,[25] S. Baroiant,[7] V. Bartsch,[31] G. Bauer,[33] P.-H. Beauchemin,[34] F. Bedeschi,[46] S. Behari,[25] G. Bellettini,[46] J. Bellinger,[59] A. Belloni,[33] D. Benjamin,[16] A. Beretvas,[17] J. Beringer,[29] T. Berry,[30] A. Bhatti,[50] M. Binkley,[17] D. Bisello,[43] I. Bizjak,[31] R.E. Blair,[2] C. Blocker,[6] B. Blumenfeld,[25] A. Bocci,[16] A. Bodek,[49] V. Boisvert,[49] G. Bolla,[48] A. Bolshov,[33] D. Bortoletto,[48] J. Boudreau,[47] A. Boveia,[10] B. Brau,[10] L. Brigliadori,[5] C. Bromberg,[36] E. Brubaker,[13] J. Budagov,[15] H.S. Budd,[49] S. Budd,[24] K. Burkett,[17] G. Busetto,[43] P. Bussey,[21] A. Buzatu,[34] K. L. Byrum,[2] S. Cabrera^{q},[16] M. Campanelli,[20] M. Campbell,[35] F. Canelli,[17] A. Canepa,[45] S. Carillo^{i},[18] D. Carlsmith,[59] R. Carosi,[46] S. Carron,[34] B. Casal,[11] M. Casarsa,[54] A. Castro,[5] P. Catastini,[46] D. Cauz,[54] M. Cavalli-Sforza,[3] A. Cerri,[29] L. Cerrito^{m},[31] S.H. Chang,[28] Y.C. Chen,[1] M. Chertok,[7] G. Chiarelli,[46] G. Chlachidze,[17] F. Chlebana,[17] I. Cho,[28] K. Cho,[28] D. Chokheli,[15] J.P. Chou,[22] G. Choudalakis,[33] S.H. Chuang,[52] K. Chung,[12] W.H. Chung,[59] Y.S. Chung,[49] M. Cilijak,[46] C.I. Ciobanu,[24] M.A. Ciocci,[46] A. Clark,[20] D. Clark,[6] M. Coca,[16] G. Compostella,[43] M.E. Convery,[50] J. Conway,[7] B. Cooper,[31] K. Copic,[35] M. Cordelli,[19] G. Cortiana,[43] F. Crescioli,[46] C. Cuenca Almenar^{q},[7] J. Cuevas^{l},[11] R. Culbertson,[17] J.C. Cully,[35] S. DaRonco,[43] M. Datta,[17] S. D'Auria,[21] T. Davies,[21] D. Dagenhart,[17] P. de Barbaro,[49] S. De Cecco,[51] A. Deisher,[29] G. De Lentdecker^{c},[49] G. De Lorenzo,[3] M. Dell'Orso,[46] F. Delli Paoli,[43] L. Demortier,[50] J. Deng,[16] M. Deninno,[5] D. De Pedis,[51] P.F. Derwent,[17] G.P. Di Giovanni,[44] C. Dionisi,[51] B. Di Ruzza,[54] J.R. Dittmann,[4] M. D'Onofrio,[3] C. Dörr,[26] S. Donati,[46] P. Dong,[8] J. Donini,[43] T. Dorigo,[43] S. Dube,[52] J. Efron,[39] R. Erbacher,[7] D. Errede,[24] S. Errede,[24] R. Eusebi,[17] H.C. Fang,[29] S. Farrington,[30] I. Fedorko,[46] W.T. Fedorko,[13] R.G. Feild,[60] M. Feindt,[26] J.P. Fernandez,[32] R. Field,[18] G. Flanagan,[48] R. Forrest,[7] S. Forrester,[7] M. Franklin,[22] J.C. Freeman,[29] I. Furic,[13] M. Gallinaro,[50] J. Galyardt,[12] J.E. Garcia,[46] F. Garberson,[10] A.F. Garfinkel,[48] C. Gay,[60] H. Gerberich,[24] D. Gerdes,[35] S. Giagu,[51] P. Giannetti,[46] K. Gibson,[47] J.L. Gimmell,[49] C. Ginsburg,[17] N. Giokaris^{a},[15] M. Giordani,[54] P. Giromini,[19] M. Giunta,[46] G. Giurgiu,[25] V. Glagolev,[15] D. Glenzinski,[17] M. Gold,[37] N. Goldschmidt,[18] J. Goldstein^{b},[42] A. Golossanov,[17] G. Gomez,[11] G. Gomez-Ceballos,[33] M. Goncharov,[53] O. González,[32] I. Gorelov,[37] A.T. Goshaw,[16] K. Goulianos,[50] A. Gresele,[43] S. Grinstein,[22] C. Grosso-Pilcher,[13] R.C. Group,[17] U. Grundler,[24] J. Guimaraes da Costa,[22] Z. Gunay-Unalan,[36] C. Haber,[29] K. Hahn,[33] S.R. Hahn,[17] E. Halkiadakis,[52] A. Hamilton,[20] B.-Y. Han,[49] J.Y. Han,[49] R. Handler,[59] F. Happacher,[19] K. Hara,[55] D. Hare,[52] M. Hare,[56] S. Harper,[42] R.F. Harr,[58] R.M. Harris,[17] M. Hartz,[47] K. Hatakeyama,[50] J. Hauser,[8] C. Hays,[42] M. Heck,[26] A. Heijboer,[45] B. Heinemann,[29] J. Heinrich,[45] C. Henderson,[33] M. Herndon,[59] J. Heuser,[26] D. Hidas,[16] C.S. Hill^{b},[10] D. Hirschbuehl,[26] A. Hocker,[17] A. Holloway,[22] S. Hou,[1] M. Houlden,[30] S.-C. Hsu,[9] B.T. Huffman,[42] R.E. Hughes,[39] U. Husemann,[60] J. Huston,[36] J. Incandela,[10] G. Introzzi,[46] M. Iori,[51] A. Ivanov,[7] B. Iyutin,[33] E. James,[17] D. Jang,[52] B. Jayatilaka,[16] D. Jeans,[51] E.J. Jeon,[28] S. Jindariani,[18] W. Johnson,[7] M. Jones,[48] K.K. Joo,[28] S.Y. Jun,[12] J.E. Jung,[28] T.R. Junk,[24] T. Kamon,[53] P.E. Karchin,[58] Y. Kato,[41] Y. Kemp,[26] R. Kephart,[17] U. Kerzel,[26] V. Khotilovich,[53] B. Kilminster,[39] D.H. Kim,[28] H.S. Kim,[28] J.E. Kim,[28] M.J. Kim,[17] S.B. Kim,[28] S.H. Kim,[55] Y.K. Kim,[13] N. Kimura,[55] L. Kirsch,[6] S. Klimenko,[18] M. Klute,[33] B. Knuteson,[33] B.R. Ko,[16] K. Kondo,[57] D.J. Kong,[28] J. Konigsberg,[18] A. Korytov,[18] A.V. Kotwal,[16] A.C. Kraan,[45] J. Kraus,[24] M. Kreps,[26] J. Kroll,[45] N. Krumnack,[4] M. Kruse,[16] V. Krutelyov,[10] T. Kubo,[55] S. E. Kuhlmann,[2] T. Kuhr,[26] N.P. Kulkarni,[58] Y. Kusakabe,[57] S. Kwang,[13] A.T. Laasanen,[48] S. Lai,[34] S. Lami,[46] S. Lammel,[17] M. Lancaster,[31] R.L. Lander,[7] K. Lannon,[39] A. Lath,[52] G. Latino,[46] I. Lazzizzera,[43] T. LeCompte,[2] J. Lee,[49] J. Lee,[28] Y.J. Lee,[28] S.W. Lee^{o},[53] R. Lefèvre,[20] N. Leonardo,[33] S. Leone,[46] S. Levy,[13] J.D. Lewis,[17] C. Lin,[60] C.S. Lin,[17] M. Lindgren,[17] E. Lipeles,[9] A. Lister,[7] D.O. Litvintsev,[17] T. Liu,[17] N.S. Lockyer,[45] A. Loginov,[60] M. Loreti,[43] R.-S. Lu,[1] D. Lucchesi,[43] P. Lujan,[29] P. Lukens,[17] G. Lungu,[18] L. Lyons,[42] J. Lys,[29] R. Lysak,[14] E. Lytken,[48] P. Mack,[26] D. MacQueen,[34] R. Madrak,[17] K. Maeshima,[17] K. Makhoul,[33] T. Maki,[23] P. Maksimovic,[25] S. Malde,[42] S. Malik,[31] G. Manca,[30] F. Margaroli,[5] R. Marginean,[17] C. Marino,[26] C.P. Marino,[24] A. Martin,[60] M. Martin,[25] V. Martin^{g},[21] M. Martínez,[3] R. Martínez-Ballarín,[32] T. Maruyama,[55] P. Mastrandrea,[51] T. Masubuchi,[55] H. Matsunaga,[55] M.E. Mattson,[58] R. Mazini,[34] P. Mazzanti,[5] K.S. McFarland,[49] P. McIntyre,[53] R. McNulty^{f},[30] A. Mehta,[30] P. Mehtala,[23] S. Menzemer^{h},[11] A. Menzione,[46] P. Merkel,[48] C. Mesropian,[50] A. Messina,[36] T. Miao,[17] N. Miladinovic,[6] J. Miles,[33] R. Miller,[36] C. Mills,[10] M. Milnik,[26] A. Mitra,[1] G. Mitselmakher,[18] A. Miyamoto,[27] S. Moed,[20] N. Moggi,[5] B. Mohr,[8] C.S. Moon,[28] R. Moore,[17]

^{24}University of Illinois, Urbana, Illinois 61801

^{25}The Johns Hopkins University, Baltimore, Maryland 21218

^{26}Institut für Experimentelle Kernphysik, Universität Karlsruhe, 76128 Karlsruhe, Germany

^{27}High Energy Accelerator Research Organization (KEK), Tsukuba, Ibaraki 305, Japan

^{28}Center for High Energy Physics: Kyungpook National University,
Taegu 702-701, Korea; Seoul National University, Seoul 151-742,
Korea; SungKyunKwan University, Suwon 440-746, Korea

^{29}Ernest Orlando Lawrence Berkeley National Laboratory, Berkeley, California 94720

^{30}University of Liverpool, Liverpool L69 7ZE, United Kingdom

^{31}University College London, London WC1E 6BT, United Kingdom

^{32}Centro de Investigaciones Energeticas Medioambientales y Tecnologicas, E-28040 Madrid, Spain

^{33}Massachusetts Institute of Technology, Cambridge, Massachusetts 02139

^{34}Institute of Particle Physics: McGill University, Montréal,
Canada H3A 2T8; and University of Toronto, Toronto, Canada M5S 1A7

^{35}University of Michigan, Ann Arbor, Michigan 48109

^{36}Michigan State University, East Lansing, Michigan 48824

^{37}University of New Mexico, Albuquerque, New Mexico 87131

^{38}Northwestern University, Evanston, Illinois 60208

^{39}The Ohio State University, Columbus, Ohio 43210

^{40}Okayama University, Okayama 700-8530, Japan

^{41}Osaka City University, Osaka 588, Japan

^{42}University of Oxford, Oxford OX1 3RH, United Kingdom

^{43}University of Padova, Istituto Nazionale di Fisica Nucleare,
Sezione di Padova-Trento, I-35131 Padova, Italy

^{44}LPNHE, Universite Pierre et Marie Curie/IN2P3-CNRS, UMR7585, Paris, F-75252 France

^{45}University of Pennsylvania, Philadelphia, Pennsylvania 19104

^{46}Istituto Nazionale di Fisica Nucleare Pisa, Universities of Pisa,
Siena and Scuola Normale Superiore, I-56127 Pisa, Italy

^{47}University of Pittsburgh, Pittsburgh, Pennsylvania 15260

^{48}Purdue University, West Lafayette, Indiana 47907

^{49}University of Rochester, Rochester, New York 14627

^{50}The Rockefeller University, New York, New York 10021

^{51}Istituto Nazionale di Fisica Nucleare, Sezione di Roma 1,
University of Rome "La Sapienza," I-00185 Roma, Italy

^{52}Rutgers University, Piscataway, New Jersey 08855

^{53}Texas A&M University, College Station, Texas 77843

^{54}Istituto Nazionale di Fisica Nucleare, University of Trieste/ Udine, Italy

^{55}University of Tsukuba, Tsukuba, Ibaraki 305, Japan

^{56}Tufts University, Medford, Massachusetts 02155

^{57}Waseda University, Tokyo 169, Japan

^{58}Wayne State University, Detroit, Michigan 48201

^{59}University of Wisconsin, Madison, Wisconsin 53706

^{60}Yale University, New Haven, Connecticut 06520

We have measured the polarizations of J/ψ and $\psi(2S)$ mesons as functions of their transverse momentum p_T when they are produced promptly in the rapidity range $|y| < 0.6$ with $p_T \geq 5$ GeV/c. The analysis is performed using a data sample with an integrated luminosity of about 800 pb^{-1} collected by the CDF II detector. For both vector mesons, we find that the polarizations become increasingly longitudinal as p_T increases from 5 to 30 GeV/c. These results are compared to the predictions of non-relativistic quantum chromo-dynamics and other contemporary models. The polarizations of J/ψ and $\psi(2S)$ mesons from B-hadron decays are also reported.

An effective field theory, non-relativistic quantum chromo-dynamics (NRQCD) [1], provides a rigorous for-

*With visitors from ^{a}University of Athens, ^{b}University of Bristol, ^{c}University Libre de Bruxelles, ^{d}Cornell University, ^{e}University of Cyprus, ^{f}University of Dublin, ^{g}University of Edinburgh, ^{h}University of Heidelberg, ^{i}Universidad Iberoamericana, ^{j}University of Manchester, ^{k}Nagasaki Institute of Applied Science, ^{l}University de Oviedo, ^{m}University of London, Queen Mary College, ^{n}University of California Santa Cruz, ^{o}Texas Tech University, ^{p}University of California Irvine, and ^{q}IFIC(CSIC-Universitat de Valencia).

malism for calculating the production rates of charmonium ($c\bar{c}$) states. NRQCD explains the direct production cross sections for J/ψ and $\psi(2S)$ mesons observed at the Tevatron [2, 3], and predicts their increasingly transverse polarizations as p_T increases [4]. The first polarization measurements at the Tevatron [5] did not show such a trend. This letter reports on J/ψ and $\psi(2S)$ polarization measurements with a larger data sample than previously available. This allows the extension of the measurement to a higher p_T region, and makes a more stringent test of the NRQCD prediction.

The NRQCD cross section calculation for $c\bar{c}$ production separates the long-distance non-perturbative contributions from the short-distance perturbative behavior. The former is treated as an expansion of the matrix elements in powers of the non-relativistic charm-quark velocity. This expansion can be computed by lattice simulations, but currently the expansion coefficients are treated as universal parameters, which are adjusted to match the cross section measurements at the Tevatron [2, 3]. The calculation also applies to $c\bar{c}$ production in ep collisions, but HERA measurements of J/ψ polarization tend to disagree with the NRQCD prediction [6]. These difficulties have led some authors to explore alternative power expansions of the long-distance interactions for the $c\bar{c}$ system [7]. There are also new QCD-inspired models, the gluon tower model [8] and the k_T-factorization model [9], that accomodate vector meson cross sections both at HERA and the Tevatron, and predict the vector meson polarizations as functions of p_T. These authors emphasize that measuring the vector meson polarizations as functions of p_T is a crucial test of NRQCD.

The CDF II detector is described in detail elsewhere [3, 10]. In this analysis, the essential features are a muon system covering the central region of pseudo-rapidity, $|\eta| < 0.6$, and the tracking system, immersed in the 1.4 T solenoidal magnetic field and comprised of a silicon micro-strip detector and a cylindrical drift chamber called the central outer tracker (COT). The data used here correspond to an integrated luminosity of about 800 pb^{-1} and were recorded between June 2004 and February 2006 by a dimuon trigger, which requires two opposite-charge muon candidates each having $p_T > 1.5$ GeV/c. Throughout this period, the COT operation was stable and the trigger efficiency did not change by more than 0.2% from the nominal value.

The trigger requirements are confirmed in offline analysis. The decays of vector mesons V (either J/ψ or $\psi(2S)) \to \mu^+\mu^-$ are selected from dimuon events for which each track has segments reconstructed in both the COT and the silicon micro-strip detector. The p_T of each muon is required to exceed 1.75 GeV/c in order to guarantee well-measured trigger efficiency. The muon track pair is required to be consistent with originating from a common vertex and to have an invariant mass M within the range 2.8 (3.4) $< M <$ 3.4 (3.9) GeV/c^2

to be considered as a J/ψ ($\psi(2S)$) candidate. To have a reasonable polarization sensitivity, the vector meson candidates are required to have $p_T \geq 5$ GeV/c in the rapidity range $|y \ (\equiv \frac{1}{2}\ln\frac{E+p_{||}}{E-p_{||}})| < 0.6$, where E is the energy and $p_{||}$ is the momentum parallel to the beam direction of the dimuon system. Events are separated into a signal region and sideband regions, as indicated in Fig. 1. The fit to the data uses a double (single) Gaussian for the J/ψ ($\psi(2S)$) signal and a linear background shape. The fits are only used to define signal and background regions. The signal regions are within $3\sigma_V$ of the fitted mass peaks M_V, where σ_V is the width obtained in the fit to the invariant mass distribution. Both the background distribution and the quantity of background events under the signal peak are estimated by events from the lower and upper mass sidebands. For J/ψ, the sideband regions are $(M_{J/\psi} - 13\sigma_{J/\psi}, \ M_{J/\psi} - 10\sigma_{J/\psi})$ and $(M_{J/\psi} + 10\sigma_{J/\psi}, \ M_{J/\psi} + 13\sigma_{J/\psi})$. For $\psi(2S)$, these are $(M_{\psi(2S)} - 10\sigma_{\psi(2S)}, \ M_{\psi(2S)} - 7\sigma_{\psi(2S)})$ and $(M_{\psi(2S)} + 7\sigma_{\psi(2S)}, \ M_{\psi(2S)} + 10\sigma_{\psi(2S)})$.
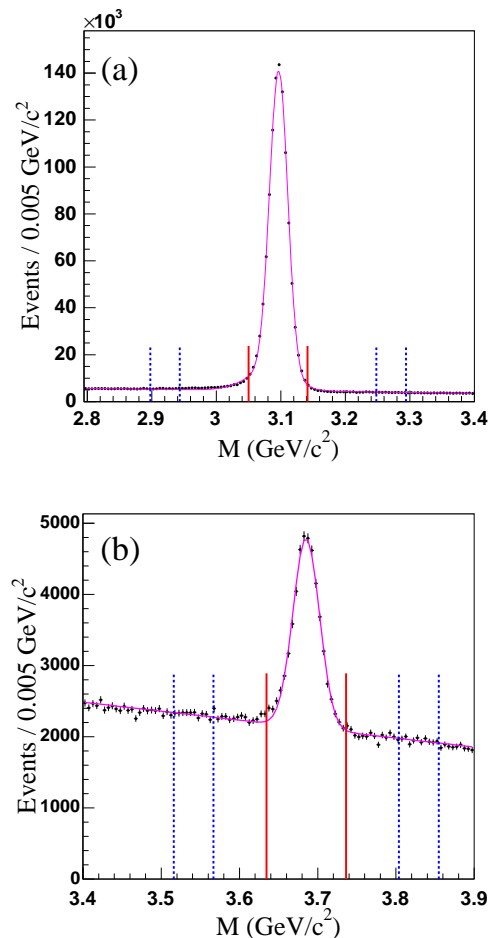

FIG. 1: Invariant mass distributions for (a) J/ψ and (b) $\psi(2S)$ candidates. The curves are fits to the data. The solid (dashed) lines indicate the signal (sideband) regions.

For each candidate, we compute $ct = ML_{xy}/p_T$, where t is the proper decay time and L_{xy} is the transverse distance between the beam line and the vector meson decay vertex measured in the plane normal to the beam direction. The ct distributions of the selected dimuon events are shown in Fig. 2. The ct distribution of prompt events is a Gaussian distribution centered at zero due to finite tracking resolution. For J/ψ, the prompt events are due to direct production or the decays of heavier charmonium states such as χ_c and $\psi(2S)$; for $\psi(2S)$, the prompt events are almost entirely due to direct production since heavier charmonium states rarely decay to $\psi(2S)$ [11]. Both the J/ψ and $\psi(2S)$ samples contain significant numbers of events originating from long-lived B-hadron decays, as can be seen from the event excess at positive ct. We have measured the fraction of $B \to J/\psi + X$ events in the J/ψ sample and found agreement with other results [3]. We select the prompt events by making a requirement on the squared sum of impact parameter significance of both the positively and negatively charged muon tracks: $S \equiv (\frac{d_0^+}{\sigma^+})^2 + (\frac{d_0^-}{\sigma^-})^2 \leq 8$, where the impact parameter d_0 is the distance of closest approach of the track to the beam line in the transverse plane. Vector meson candidates from B-hadron decays are selected by requiring $S > 16$ and $ct > 0.03$ cm. This requirement retains a negligible fraction of prompt events in the B sample.

The goal of this analysis is to measure the polarizations of prompt J/ψ and $\psi(2S)$ mesons as functions of p_T. As shown in Table I, the J/ψ events are analyzed in six p_T bins; there are about 30 times fewer $\psi(2S)$ events, so we use three bins. After the prompt event selection requirement $S \leq 8$, we determine the fraction of B-decay background remaining in prompt samples, f_{bkd}, by subtracting the number of negative ct events from the number of positive ct events. Only a negligible fraction ($< 0.2\%$) of B decays produce vector meson events with negative ct. For both vector mesons, f_{bkd} increases with p_T, as listed in Table I. The prompt polarization from the fitting algorithm is corrected for this contamination.

The polarization information is contained in the distribution of the muon decay angle θ^*, the angle of the μ^+ in the rest frame of vector meson with respect to the vector-meson boost direction in the laboratory system. The decay angle distribution depends on the polarization parameter α: $\frac{dN}{d\cos\theta^*} \propto 1 + \alpha \cos^2\theta^*$ ($-1 \leq \alpha \leq 1$). For fully transverse (longitudinal) polarization, $\alpha = +1 (-1)$. Intermediate values of α indicate a mixture of transverse and longitudinal polarization.

A template method is used to account for acceptance and efficiency. Two sets of $\cos\theta^*$ distributions for fully-polarized decays of J/ψ and $\psi(2S)$ events, one longitudinal (L) and the other transverse (T), are produced with the CDF simulation program using the efficiency-corrected p_T spectra measured from data [3, 12]. We use the muon trigger efficiency measured using data as a
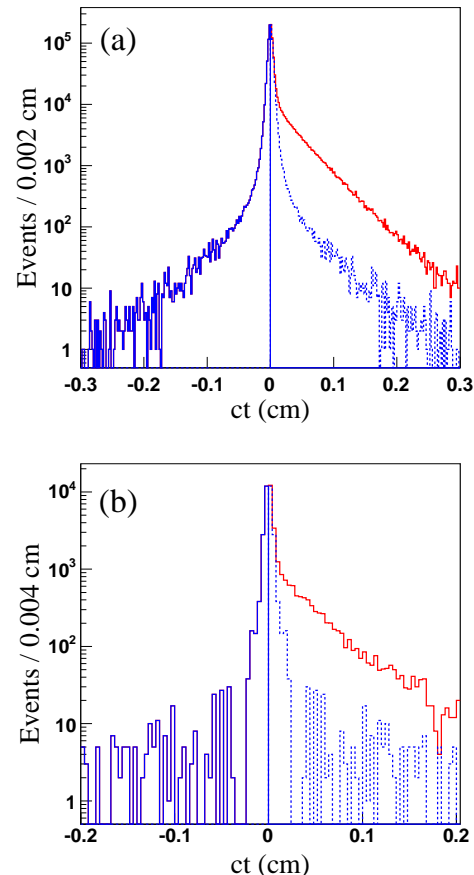

FIG. 2: Sideband-subtracted ct distributions for (a) J/ψ and (b) $\psi(2S)$ events. The prompt Gaussian peak, positive excess from B-hadron decays, and negative tail from mismeasured events are shown. The dotted line is the reflection of the negative ct histogram about zero.

function of track parameters (p_T, η, ϕ) to account for detector non-uniformities. The parameterized efficiency is used as a filter on all simulated muons. Events that pass reconstruction represent the behavior of fully-polarized vector meson decays in the detector.

The fitting algorithm [5] uses two binned $\cos\theta^*$ distributions for each p_T bin, one made by N_S events from the signal region (signal plus background) and the other made by N_B events from the sideband regions (background). The χ^2 minimization is done simultaneously for both $\cos\theta^*$ distributions. The expected signal distribution is a polarization-weighted linear combination of the L and T templates, normalized to $N_S - N_B$. The fitting algorithm includes an individual background term for each $\cos\theta^*$ bin, normalized to N_B. Simulation shows that the $\cos\theta^*$ resolution at all decay angles over the entire p_T range is much smaller than the bin width of 0.05 (0.10 for $\psi(2S)$) used here. The fitting algorithm is verified on a set of simulated samples with polarizations ranging from -1 to $+1$ in steps of 0.2.

Many possible sources of systematic uncertainties were examined. All systematic uncertainties are much smaller than the statistical uncertainties. When the p_T spectrum used in the simulation was varied within 1σ uncertainties and the templates were reweighted to reflect the changes in acceptance, the polarization parameter for J/ψ varied at most by 0.002. A systematic uncertainty of 0.007 was estimated by the change in the polarization parameter when a modification was made on all trigger efficiencies by $\pm 1\sigma$. For $\psi(2S)$, the dominant systematic uncertainty came from the yield estimate because of the radiative tail and the large background. The total systematic uncertainties shown in Table I were taken to be the quadrature sum of these individual uncertainties. Other possible sources of systematic uncertainties were determined to be negligible. The method of extracting the signal and background $\cos\theta^*$ distributions by a mass fit in each $\cos\theta^*$ bin gave consistent polarization results. The polarization results were not affected by different choices of $\cos\theta^*$ bin size. The corrections to prompt polarization from B-decay contamination were small, so that uncertainties on B-decay polarization measurements had also negligible effect. The ϕ-dependence of polarizations was checked and no effects were found.

The polarization of J/ψ mesons from inclusive B_u and B_d decays was measured by the $BABAR$ collaboration [13]. In this analysis, the B-hadron direction is unknown, so we define θ^* with respect to the J/ψ direction in the laboratory system. The resulting polarization is somewhat diluted. As discussed in Ref. [3], CDF uses a Monte Carlo procedure to adapt the $BABAR$ measurement to predict the effective J/ψ polarization parameter. For the J/ψ events with $5 \leq p_T < 30$ GeV/c, the CDF model for B_u and B_d decays gives $\alpha_{eff} = -0.145 \pm 0.009$, independent of p_T. We have measured the polarization of vector mesons from B-hadron decays. For J/ψ, we find $\alpha_{eff} = -0.106 \pm 0.033$ (stat) ± 0.007 (syst). At this level of accuracy a polarization contribution by J/ψ mesons from B_s and b-baryon decays cannot be separated from the effective polarization due to those from B_u and B_d decays. We also report the first measurement of the $\psi(2S)$ polarization from B-hadron decays: $\alpha_{eff} = 0.36 \pm 0.25$ (stat) ± 0.03 (syst).

The polarization parameters for both prompt vector mesons corrected for f_{bkd} using our experimental results on α_{eff} are listed as functions of p_T in Table I and are plotted in Fig. 3. The polarization parameters for J/ψ are negative over the entire p_T range of measurement and become increasingly negative (favoring longitudinal polarization) as p_T increases. For $\psi(2S)$, the central value of the polarization parameter is positive at small p_T, but given the uncertainties its behavior is consistent with the trend shown in the measurement of the J/ψ polarization. The polarization behavior measured previously with 110 pb^{-1} [5] is not consistent with the results presented here. We have searched for the source of this

inconsistency to the extent possible, but have been unable to determine any specific cause. The measurements presented here supersede the results of Ref. [5].
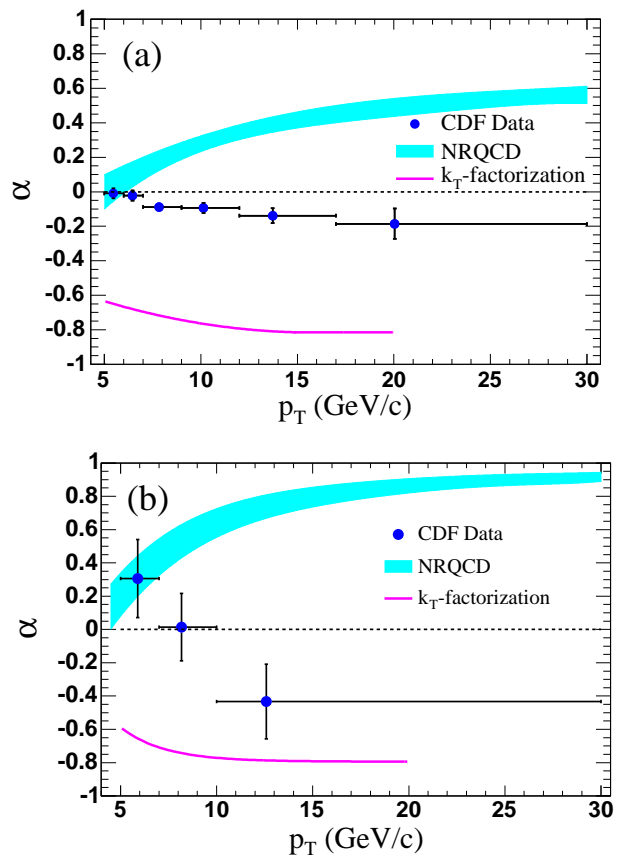

FIG. 3: Prompt polarizations as functions of p_T: (a) J/ψ and (b) $\psi(2S)$. The band (line) is the prediction from NRQCD [4] (the k_T-factorization model [9]).

These polarization measurements for the charmed vector mesons extend to a p_T regime where perturbative QCD should be applicable. The results are compared to the predictions of NRQCD and the k_T-factorization model in Fig. 3. The prediction of the k_T-factorization model is presented for $p_T < 20$ GeV/c and does not include the contribution from the decays of heavier charmonium states for J/ψ production. The polarizations for prompt production of both vector mesons become increasingly longitudinal as p_T increases beyond 10 GeV/c. This behavior is in strong disagreement with the NRQCD prediction of large transverse polarization at high p_T. Although the NRQCD calculation successfully reproduces the measured J/ψ and $\psi(2S)$ cross sections at the Tevatron, its disagreement with these polarization measurements indicates that there is some aspect of the production mechanism that is not yet understood. Further studies of this feature of the process may lead to important new insight into the hadroproduction of charmonium.

	p_T (GeV/c)	$<p_T>$ (GeV/c)	f_{bkd} (%)	α	χ^2/d.o.f
J/ψ	$5-6$	5.5	2.8 ± 0.2	$-0.009 \pm 0.029 \pm 0.007$	21.4/22
	$6-7$	6.5	3.4 ± 0.2	$-0.022 \pm 0.028 \pm 0.007$	31.0/24
	$7-9$	7.8	4.1 ± 0.2	$-0.088 \pm 0.023 \pm 0.007$	46.7/27
	$9-12$	10.1	5.7 ± 0.3	$-0.094 \pm 0.028 \pm 0.007$	34.2/30
	$12-17$	13.7	6.7 ± 0.6	$-0.139 \pm 0.043 \pm 0.007$	38.3/32
	$17-30$	20.0	13.6 ± 1.4	$-0.187 \pm 0.090 \pm 0.007$	33.9/34
$\psi(2S)$	$5-7$	5.9	1.6 ± 0.9	$+0.306 \pm 0.235 \pm 0.027$	14.4/12
	$7-10$	8.2	4.9 ± 1.2	$+0.014 \pm 0.202 \pm 0.023$	18.7/14
	$10-30$	12.6	8.6 ± 1.8	$-0.433 \pm 0.224 \pm 0.016$	26.8/16

TABLE I: Polarization parameter α for prompt production in each p_T bin. The first (second) uncertainty is statistical (systematic). $<p_T>$ is the average transverse momentum.

[1] G. T. Bodwin, E. Braaten, and G. P. LePage, Phys. Rev. D **51**, 1125 (1995); Erratum, *ibid*. Phys. Rev. D **55**, 5853 (1997); E. Braaten and S. Fleming, Phys. Rev. Lett. **74**, 3327 (1995).

[2] F. Abe *et al.* (CDF Collaboration), Phys. Rev. Lett. **79**, 572 (1997).

[3] D. Acosta *et al.* (CDF Collaboration), Phys. Rev. D **71**, 032001 (2005).

[4] P. Cho and M. Wise, Phys. Lett. B **346**, 129 (1995); M. Beneke and I. Z. Rothstein, Phys. Lett. B **372**, 157 (1996); Erratum, *ibid*. Phys. Lett. B **389**, 769 (1996); E. Braaten, B. A. Kniehl, and J. Lee, Phys. Rev. D **62**, 094005 (2000).

[5] T. Affolder *et al.* (CDF Collaboration), Phys. Rev. Lett. **85**, 2886 (2000).

[6] C. Adloff *et al.* (H1 Collaboration), Eur. Phys. J. C **25**, 41 (2002); S. Chekanov *et al.* (ZEUS Collaboration), Eur. Phys. J. C **44**, 13 (2005).

[7] S. Fleming, I. Z. Rothstein, and A. K. Leibovich, Phys. Rev. D **64**, 036002 (2001).

[8] V. A. Khoze, A. D. Martin, M. G. Ryskin, and W. J. Stirling, Eur. Phys. J. C **39**, 163 (2005).

[9] S. P. Baranov, Phys. Rev. D **66**, 114003 (2002).

[10] The CDF coordinate system has $\hat{z}$ along the proton direction, $\hat{x}$ horizontal pointing outward from the Tevatron ring, and $\hat{y}$ vertical. θ (ϕ) is the polar (azimuthal) angle measured with respect to $\hat{z}$ and η is the pseudorapidity defined as $-\ln(\tan(\theta/2))$. The transverse momentum of a particle is denoted as $p_T = p\sin\theta$.

[11] W.-M. Yao *et al.* (Particle Data Group), J. Phys. G **33**, 1 (2006).

[12] A letter on $\psi(2S)$ cross section measurement is under preparation.

[13] B. Aubert *et al.* (*BABAR* Collaboration), Phys. Rev. D **67**, 032002 (2003).